Theoretical Investigations of the Gas-Phase Dimers (CH_4, HX), X = F, Cl, Br

Asit K. Chandra* and Minh Tho Nguyen*

Department of Chemistry, University of Leuven, Celestijnenlaan 200F, B-3001 Leuven, Belgium

Received: April 8, 1998; In Final Form: June 5, 1998

Ab initio calculations have been carried out at the MP2=full level with 6-311++G(3df,2p) basis functions to determine the equilibrium geometries and binding energies of the 1:1 gas-phase complexes between CH_4 and HX (X = F, Cl, Br). Single-point MP4 calculation at the MP2 optimized geometry has also been performed to include the effect of higher order electron correlation in the binding energy. Contrary to the earlier experimental and low-level theoretical investigations, it is observed that the nonconventional hydrogen-bonded structure is the most stable complex for all the three hydrogen halides. This occurs when the proton of HX forms a weak hydrogen bond to the center of one of the methane tetrahedral faces to form a symmetric top C_{3v} dimer. Symmetry-adapted perturbation theory (SAPT) analysis has been carried out to understand the nature of the forces involved in the bonding and also to examine how different interaction energy components vary with the change in intermolecular distance. It has been observed that the binding energy of the (CH_4, HX) dimer decreases in the order HF > HCl > HBr.

1. Introduction

The complexes between methane and hydrogen halides are of recent experimental and theoretical interest.[1−5] From the pulsed-nozzle Fourier transform microwave spectroscopy, Legon and co-workers[2] observed that the equilibrium structure of the (CH_4, HF) dimer is different from the equilibrium structure of the (CH_4, HCl) and (CH_4, HBr)[4] dimers. In the case of the HF complex, the equilibrium structure is a conventional hydrogen-bonded structure, where the fluorine atom of HF forms a weak bond with the hydrogen atom of CH_4 (structure a of Figure 1), whereas in the case of HCl and HBr, it is the nonconventional structure, b in Figure 1, which is the most stable. The proton of HCl or HBr forms a weak hydrogen bond to the center of one of the methane tetrahedral faces to yield a symmetric top C_{3v} dimer $CH_4\cdots HX$. Similar observation was made earlier by Davis and Andrews[1] from infrared spectroscopy experiments on noble gas matrixes and ab initio calculations at the Hartree−Fock level with 6-31G(d,p) basis functions. Subsequent theoretical calculations by Nguyen et al.[6] at the MP2/6-311G(d,p) level of theory supported the observations made from the experiment about the contrasting behavior of (CH_4, HF) and (CH_4, HCl) dimers.

However, the theoretical calculations at the said level fail to explain the observed low-frequency shift of the H−X stretching vibration in the complex compared to the free HX. Moreover, Legon and co-workers[2] estimated that the (CH_4, HF) dimer should have a greater binding strength than the (CH_4, HCl) dimer, whereas theoretical calculations at MP2/6-311G(d,p) predict a much weaker HF complex compared to the HCl complex. Thus experiment and theoretical calculations at the MP2/6-311G(d,p) level predict the same overall optimum geometry of the (CH_4, HF) dimer. But, they differ significantly with respect to the other observations mentioned above. These disagreements between experiment and theoretical calculations might have two origins. First, to obtain a reasonable equilibrium structure for a very weak complex, one needs to include electron correlation and a basis set that is flexible enough to take care of all the important interaction energy components. Second, the experimental geometry is always vibrationally averaged, and thus one-to-one comparison between experiment and theoretical calculation does not make any sense. Now, the basis sets used in earlier theoretical studies are obviously not suitable for studying a weak molecular complex. It is well-known that diffuse functions and multiple polarization functions are indispensable for the study of weak complexes.[7] Moreover, anticipating that the dispersion energy might play an important role in these weak complexes, it is necessary to include higher angular momentum polarization functions in the basis set. In view of the above-mentioned disagreement between theoretical and experimental observations for the (CH_4, HF) complex, we feel that it is necessary to study this system by more accurate theoretical techniques. In addition, present study has been extended to the HCl and HBr complexes with CH_4 at the same level of theory for a reasonable comparison of these complexes. To our knowledge, there has been no theoretical study to date on the (CH_4, HBr) system. Interaction energy component analysis based on symmetry-adapted perturbation theory (SAPT)

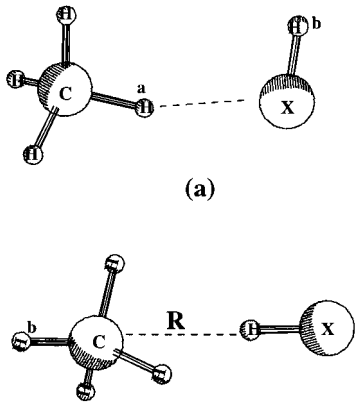

Figure 1. Possible structures for the (CH_4, HX) dimers, X = F, Cl, Br.

* Corresponding author. Email: asit.chandra@chem.kuleuven.ac.be. Fax: 32-16-327992.

S1089-5639(98)01814-3 CCC: $15.00
Published on Web 07/31/1998

has been performed to understand the forces involved in these dimers and how they differ from one complex to the other. Moreover, SAPT analysis has also been performed for both conventional and nonconventional forms of the (CH_4, HF) dimer to understand how they differ in the nature of interaction.

2. Computational Details

Geometries of the monomers, CH_4 and HX (X = F, Cl, Br), and dimers (CH_4, HX) were fully optimized at second-order Moller−Plesset perturbation theory (MP2) level including all the electrons and using two basis sets: 6-311++G(d,p) and 6-311++G(3df,2p). The basis sets were taken directly from the Gaussian program library. Harmonic vibrational frequencies were calculated at the same level of theory and using the same basis set to characterize the stationary point and to calculate the frequency shift due to complex formation. Single-point MP4=full/6-311++G(3df,2p)//MP2=full/6-311++G(3df,2p) calculations were also performed for the HF and HCl complexes with CH_4 to include the higher order electron correlation effect on binding energy. MP4 calculations for the HBr complex could not be performed owing to limitations in our computer resources. Single-point MP2=full/6-311++G(3df,2pd) calculations using *f*- and *d*-exponents as proposed in ref 7 (f(C) = 0.11, f(F) = 0.275, f(Cl) = 0.15, and d(H) = 0.12) were also performed on (CH_4, HF) and (CH_4, HCl) dimers. All the supermolecular ab initio calculations were performed by using the Gaussian 94 program.[8] Interaction energy component analysis was performed by following the technique of symmetry-adapted perturbation theory (SAPT),[9,10] and calculations were done by using the SAPT program.[11] Basis set superposition error was estimated by the counterpoise (CP) method of Boys and Bernardi.[12]

3. Results and Discussion

3.1. Structure and Energetics. Although there are many possible structures for the dimeric systems (CH_4, HX), earlier theoretical[6] and experimental studies[1−3] identified the structures a and b in Figure 1 are the most probable structures for these complexes. The present study is restricted to these two forms. Experimental studies predicted that the structure of the (CH_4, HF) dimer is similar to the structure in Figure 1a with a conventional hydrogen bond between the fluorine atom of HF and the hydrogen of CH_4. Similar conclusions were reached by theoretical calculations at the MP2/6-311G(d,p) level.[6] Contrary to these observations, our calculations at the MP2=full/6-311++G(3df,2p) level show that the nonconventional structure (structure b in Figure 1) is much more stable than the conventional one for the (CH_4, HF) dimer. In fact, the structure a is found to be a transition state with one negative frequency and energetically far less stable (by 0.99 kcal/mol) than the structure b. Single-point MP2=full/6-311++G(3df,2pd) calculations using *f*- and *d*-exponents as proposed by Chalasinski and Szczesniak[7] for better estimation of dispersion energy show structure b is 1.00 kcal/mol more stable than structure a. The optimized $H_a\cdots X$ distance in structure a is 2.72 Å, and the distance between the carbon atom and the hydrogen atom of HF is found to be 4.30 Å. These geometrical parameters are not much different from those predicted by Davis and Andrews,[1] but they differ significantly from those obtained by Nguyen et al.[6] and Legon and co-workers.[2] Structure b, where the proton of HF forms a weak bond to the center of one of the tetrahedral faces with a near C_{3v} symmetry, is thus found to be the most stable structure for the (CH_4, HF) dimer. Similar observations were also made from the MP2=full/6-311++G(d,p) level of theory. Several geometry optimizations for the (CH_4, HF) dimer starting from a geometry predicted by Legon and co-workers[2] using different basis sets were performed. But any stationary point similar in geometry to that predicted by these authors could not be located. The equilibrium structures for the (CH_4, HCl) and (CH_4, HBr) dimers are like that shown in Figure 1b, which are also similar to that predicted from the experiments. Thus all the three hydrogen halides form nonconventional hydrogen-bonded complex with CH_4.

TABLE 1: Optimum Hydrogen Bond Length, *R* (See Structure b in Figure 1), Dipole Moment (μ in D), and Rotational Constants (*B* and *C* in GHz) Obtained from the MP2=full/6-311++G(3df,2p) Calculations for the (CH_4, HX) Dimers[a]

complex	*R* (Å)	μ	rotational constant
CH_4−HF	2.33 (2.51)	2.28	5.299 68 (4.774 05)
			5.299 65 (4.773 66)
CH_4−HCl	2.49 (2.68)	1.46	3.186 43 (2.942 39)
			3.186 41 (2.941 36)
CH_4−HBr	2.56 (2.76)	1.22	2.360 66 (2.203 29)
			2.360 63 (2.202 41)

[a] The quantities in parentheses are those obtained from the MP2=full/6-311++G(d,p) level of theory. Monomer geometrical parameters at the MP2=full//6-311++G(3df,2p) level are C−H, 1.084 Å; H−F, 0.9173 Å; H−Cl, 1.2715 Å; and H−Br, 1.4122 Å.

TABLE 2: Binding Energies (kcal/mol) without (ΔE) and with (ΔE_c) BSSE Correction, ΔZPVE (kcal/mol), and Low-Frequency Shift ($\Delta\nu$ in cm^{-1}) in the H−X Stretching Vibration As Obtained from Supermolecular MP2=full/6-311++G(3df,2p) Calculations for the Structure b in Figure 1[a]

complex (structure)	MP2			MP4		
	ΔE^b	ΔE_c	ΔZPVE	ΔE	ΔE_c	$\Delta\nu^c$
CH_4−HF(b)	1.84	1.27	1.22	1.89	1.30	42
	[2.14][d]	[1.31]				
	(1.43)	(0.73)	(1.28)			(39)
CH_4−HF(a)	0.42	0.28				
	[0.75][d]	[0.31]				
	(0.50)	(0.14)				
CH_4−HCl(b)	1.57	0.97	0.90	1.47	0.85	17
	[3.05][d]	[1.04]				
	(1.24)	(0.46)	(0.80)			(04)
CH_4−HBr(b)	1.34	0.43	0.75			08
	(1.07)	(0.62)	(0.69)			(03)

[a] Binding energy of the structure a in Figure 1 of the CH_4−HF dimer is also included in the table. Values in parentheses are those obtained from the MP2=full/6-311++G(d,p) level. MP4=full/6-311++G(3df,2p) calculations were carried out at the optimized geometry obtained at the MP2=level of theory. [b] $\Delta E = E_A + E_B - E_{AB}$. [c] Frequencies at the MP2 level of theory. [d] Obtained from single-point calculations at the MP2=full/6-311++G(3df,2pd) level using the following *f*- and *d*-function exponents for heavy atoms and H-atom, respectively: f(C) = 0.11, f(F) = 0.275, f(Cl) = 0.15, and d(H) = 0.12.

Tables 1 and 2 show the optimized intermolecular distance (*R* in structure b of Figure 1), rotational constants, binding energies, and H−X stretching vibrational frequency shift in the complex for all the three (CH_4, HX) dimers. The most striking observation from Table 1 is the change in the equilibrium intermolecular distance *R* with the change of basis functions from 6-311++G(d,p) to 6-311++G(3df,2p). The addition of extra polarization functions in the basis set brings the two monomers closer to each other by almost 0.2 Å. This is surely due to the fact that the dispersion energy is better estimated in the case of 6-311++G(3df,2p) basis set, which will be more clear when we look at SAPT energy component analysis in the next section. To test the convergence of the optimum intermolecular distance *R* (Figure 1b) with respect to the basis size,

additional geometry optimizations were performed at the MP2 level for the structure b of CH_4-HF using 6-311++G(2d,2p), 6-311++G(2df,2p), and 6-311++G(2df,2pd) basis sets. It has been observed that the distance R varies within 2.30 to 2.32 Å. The optimum intermolecular distance (R_o) of the (CH_4, HX) complexes increases in the order HF < HCl < HBr. The C···X distances obtained from the experiment for the HCl and HBr complexes are 3.9376 and 4.14 Å, respectively, whereas the theoretical values obtained at the MP2=full/6-311++G(d,p) level are 3.9148 and 4.115 Å and those at MP2=full/6-311++G(3df,2p) level are 3.7589 and 3.974 Å for the HCl and HBr complexes, respectively. As mentioned earlier the experimental geometries are vibrationally averaged and are, thus, not directly comparable with the theoretical values. It is expected that not-removed BSSE during supermolecular calculations also shortens the intermolecular distance R. To check this effect, several single-point calculations were performed around the supermolecular optimized value of R (2.33 Å) for the CH_4-HF system. It was observed that the BSSE corrected supermolecular interaction energy attains its maximum value at $R =$ 2.37 Å, which is 0.04 Å longer than the optimum value of R obtained from the supermolecular calculations. However, it is clear that the intermolecular distances obtained from larger basis set calculations are shorter than the experimental values, whereas those obtained from the smaller basis set are fairly closer to the experiment. Rotational constants are also significantly different from those obtained from the experiment. Monomer geometries are found to be virtually unchanged in the complex. The highest change observed for the H−F bond length in the (CH_4, HF) dimer amounts to 0.002 Å. In all the (CH_4, HX) complexes, the C−H_b (see structure b in Figure 1) distance is found to be same as the C−H distance in free CH_4, whereas the other three C−H bonds increase by an amount of 0.001 Å in the complex.

It is clear from Table 2 that the binding energies of these complexes decrease in the order HF > HCl > HBr. The same trend was predicted by Legon and co-workers.[2] However, if one assumes a bent geometry (structure a in Figure 1) for the (CH_4, HF) dimer, then the HCl complex is more stable than the HF complex. This is the reason Nguyen et al.[6] had obtained the HCl complex as far more stable than the HF complex. Table 2 also shows that use of *f*- and *d*-exponents for heavy atoms and H-atom as proposed in ref 7 for better estimation of dispersion energy has very little effect on the binding energies obtained by using the 6-311++G(3df,2p) basis taken directly from the Gaussian library. MP4 results are also included in the Table 2. It is clear that there is no significant effect of higher order electron correlation on the binding energies of these complexes.

In matrix isolation experiment, Davis and Andrews[1] observed a downshift of 23 cm^{-1} in the H−F stretching vibration following complex formation, whereas Paulson and Barnes[13] noticed a downshift of 16 cm^{-1} in the H−Cl stretching mode. MP2/6-311G(d,p) calculations show a reverse trend.[6] However, present calculations indeed show a low shift of H−X stretching frequency due to complex formation with CH_4. The shifts obtained from our best calculations are 42, 17, and 8 cm^{-1} for the HF, HCl, and HBr, respectively. The experimental vibrational frequency includes the effect of anharmonicity and are, thus, not comparable with the frequencies obtained from harmonic approximations. However, if we assume that anharmonicity would be same in free H−X and in the complex, then harmonic shift should provide an estimate of the frequency shift due to complex formation. The low-frequency shifts are more

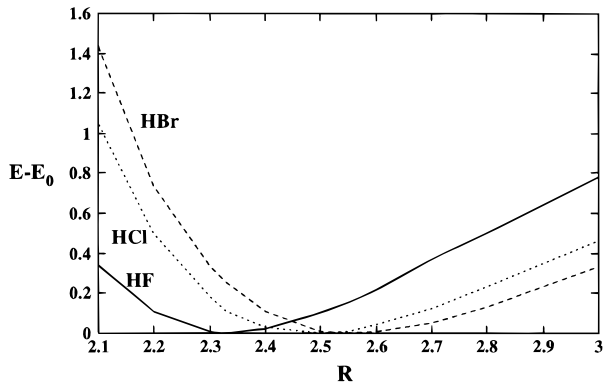

Figure 2. Change in relative energy ($E - E_o$ in kcal/mol) with the change in intermolecular distance R (in Å) for the CH_4-HX (X = F, Cl, Br) complexes. Energies are calculated at the MP2=full level with 6-311++G(3df,2p) basis functions.

at the MP2=full/6-311++G(3df,2p) level compared to those obtained from the MP2=full/6-311++G(d,p) calculations. For a particular basis set, the H−X frequency shift decreases in the order HF > HCl> HBr, which is also the order of their interaction energy with CH_4. It was also observed from our calculations that IR-inactive C−H stretching vibration of CH_4 becomes weakly active in the complex and the transition intensity is highest for the (CH_4, HF) dimer. This shows that the HF ligand produces enough asymmetry in the CH_4 molecule of the complex to make the C−H stretching mode weakly active. The frequencies related to the various vibrational modes of the CH_4 submolecule in the (CH_4, HX) complexes remain virtually unchanged to the corresponding free CH_4 values.

Figure 2 displays the intermolecular potential for the (CH_4, HX) dimers. The potential has been calculated at the MP2=full/6-311++G(3df,2p) level and keeping all the geometrical parameters but R (Figure 1b) fixed at the respective optimized values.

3.2. SAPT Analysis. A partitioning of the interaction energy into various physically meaningful parts such as electrostatic, exchange repulsion, induction, and dispersion has been performed using the symmetry-adapted perturbation theory (SAPT).[10] Only a brief description of the approach is given here in order to clarify the points relevant to the present calculations (for details about the SAPT approach, see refs 14−16). The interaction energy in SAPT is defined directly[10] as the sum of physically distinct *polarization* and *exchange* contributions

$$E_{\text{int}} = E_{\text{pol}}^{(1)} + E_{\text{exch}}^{(1)} + E_{\text{pol}}^{(2)} + E_{\text{exch}}^{(2)} + \cdots$$

where $E_{\text{pol}}^{(1)}$ is the classical *electrostatic* energy and $E_{\text{pol}}^{(2)}$ is the sum of classical *induction* and quantum mechanical *dispersion* energies and $E_{\text{exch}}^{(n)}$, $n = 1, 2$, are exchange corrections. The latter represents the effect of the resonance tunneling of electrons between the interacting systems.

Electron correlation effects on the first-order exchange contribution were approximated by

$$\epsilon_{\text{exch}}^{(1)} = E_{\text{exch}}^{(11)} + E_{\text{exch}}^{(12)} + \Delta_{\text{exch}}^{(1)}(\text{CCSD})$$

The first and second-order cluster operators in the expression for $E_{\text{exch}}^{(12)}$ are replaced by converged coupled-cluster operators,[17] leading to a sum of higher order terms (in terms of intramolecular correlation) denoted by $\Delta_{\text{exch}}^{(1)}(\text{CCSD})$. The effect of monomer electron correlation on electrostatic interaction is estimated up to third order and expressed as

$$\epsilon_{pol}^{(1)} = E_{pol,resp}^{(12)} + E_{pol,resp}^{(13)}$$

The interaction energies were calculated using the following approximations:

$$E_{pol} = E_{pol}^{(10)} + \epsilon_{pol}^{(1)}$$

$$E_{exch}^{(1)} = E_{exch}^{(10)} + E_{exch}^{(11)} + E_{exch}^{(12)} + \Delta_{exch}^{(1)}(CCSD)$$

$$E_{ind}^{(2)} = E_{ind,resp}^{(20)} + E_{ind}^{(22)}$$

$$E_{exch-ind}^{(2)} = E_{exch-ind.resp}^{(20)} + E_{exch-ind}^{(22)}$$

$$E_{disp} = E_{disp}^{(20)} + E_{disp}^{(21)} + E_{disp}^{(22)}$$

$$E_{exch-disp}^{(2)} = E_{exch-disp}^{(20)}$$

Superscripts (*ij*) in the above expressions refer to the order of the intermolecular interaction operator and the intramolecular correlation operator, respectively (see ref 10 for more details). Present SAPT calculations were terminated at second order with respect to the intermolecular interaction potential. Induction and dispersion components were estimated up to second order of monomer correlation. The total interaction energy of the complex can be estimated as[18]

$$E_{int}^{tot} = E_{int}^{HF} + E_{int}^{corr}$$

where E_{int}^{HF} is the supermolecular Hartree−Fock interaction energy and in the present calculation E_{int}^{corr} is expressed as

$$E_{int}^{corr} = E_{pol,resp}^{(12)} + E_{pol,resp}^{(13)} + E_{ind}^{(22)} + E_{ex-ind}^{(22)} + E_{exch}^{(1)} + \epsilon_{exch}^{(1)} + E_{disp}^{(2)} + E_{ex-disp}^{(20)}$$

These expansions account for the so-called *response* for the perturbation-induced modification of the molecular orbitals.[18] E_{int}^{HF} were calculated with dimer-centered basis set to avoid any BSSE. The present SAPT calculations for the (CH_4, HF) and (CH_4, HCl) dimers were performed by using the 6-311++G-(2df,2p) basis functions. The monomer geometries used in the SAPT calculations are C−H, 1.0826 Å; H−F, 0.9173 Å; H−Cl, 1.2696 Å. The calculations were performed at various values of *R* for the structure b in Figure 1. The same analysis for the HBr complex could not be performed owing to limitations in our computer resources. However, we observed from the SAPT analysis using smaller basis functions such as 6-311++G(d,p) that the general trend of various energy components is the same for the HCl and HBr complexes of CH_4.

Tables 3 and 4 present the various interaction energy components for the HF and HCl complexes of methane at different values of *R*. At shorter *R*, the repulsive exchange interactions are more for the HCl complex and they decay faster than the HF complex. Induction forces are not much different for the two complexes, and they decay almost in a similar way with the increase in *R*. $E_{pol}^{(10)}$ is significantly larger for the HCl complex when $R < R_o$ (R_o is the optimum value of *R*). It decays faster than for the HF complex, and the difference between them is very small at $R \gg R_o$. Compared to the HF complex, the dispersion components are substantially larger for the HCl complex, particularly at smaller *R*. For both the complexes, dispersion is the major attractive force at equilibrium. At equilibrium ($R = 2.60$ Å), the CH_4−HCl complex is repulsive at the Hartree−Fock level and the whole stabilization energy

TABLE 3: Components of Interaction Energy (in kcal/mol) as Functions of the Intermolecular Distance *R* (See Structure b in Figure 1) for the CH_4−HF Complex[a]

	R (Å)						
	2.10	2.30	2.40	2.50	2.60	2.80	3.00
E_{pol}^{10}	−1.76	−1.13	−0.93	−0.76	−0.64	−0.45	−0.34
E_{exch}^{10}	4.85	2.34	1.62	1.12	0.77	0.37	0.17
$E_{ind,resp}^{20}$	−2.67	−1.45	−1.09	−0.82	−0.63	−0.37	−0.23
E_{ex-ind}^{20}	1.13	0.51	0.34	0.23	0.16	0.07	0.03
E_{int}^{HF}	0.93	−0.04	−0.26	−0.38	−0.44	−0.43	−0.39
$\epsilon_{exch}^{(1)}$	0.81	0.44	0.32	0.23	0.17	0.09	0.04
$\epsilon_{pol}^{(1)}$	−0.31	−0.17	−0.13	−0.10	−0.08	−0.05	−0.03
$E_{ex-disp}^{20}$	0.25	0.13	0.09	0.06	0.04	0.02	0.01
E_{disp}^{2}	−2.29	−1.48	−1.19	−0.96	−0.78	−0.52	−0.35
E_{int}^{corr}	−1.60	−1.11	−0.93	−0.77	−0.65	−0.45	−0.32
E_{int}^{tot}	−0.67	−1.15	−1.19	−1.15	−1.08	−0.89	−0.71
E_{int}^{sm}			−1.18				

[a] BSSE corrected supermolecular interaction energy (E_{int}^{sm}) at the MP2=full/6-311++G(2df,2p) level is also given in the table.

TABLE 4: Components of Interaction Energy (in kcal/mol) as Functions of the Intermolecular Distance *R* (See Structure b in Figure 1) for the CH_4−HCl Complex[a]

	R (Å)						
	2.10	2.30	2.40	2.50	2.60	2.80	3.00
E_{pol}^{10}	−2.70	−1.55	−1.19	−0.92	−0.72	−0.47	−0.32
E_{exch}^{10}	8.28	4.18	2.95	2.08	1.46	0.72	0.35
$E_{ind,resp}^{20}$	−2.91	−1.44	−1.02	−0.73	−0.53	−0.29	−0.16
E_{ex-ind}^{20}	1.78	0.80	0.53	0.35	0.23	0.10	0.05
E_{int}^{HF}	3.39	1.44	0.89	0.51	0.25	−0.02	−0.13
$\epsilon_{exch}^{(1)}$	0.69	0.40	0.30	0.22	0.17	0.09	0.05
$\epsilon_{pol}^{(1)}$	−0.29	−0.16	−0.12	−0.10	−0.07	−0.04	−0.03
$E_{ex-disp}^{20}$	0.49	0.27	0.20	0.15	0.10	0.05	0.03
E_{disp}^{2}	−3.60	−2.37	−1.93	−1.57	−1.28	−0.86	−0.59
E_{int}^{corr}	−2.75	−1.89	−1.57	−1.31	−1.10	−0.77	−0.54
E_{int}^{tot}	0.63	−0.45	−0.68	−0.80	−0.85	−0.79	−0.68
E_{int}^{sm}					−0.88		

[a] BSSE corrected supermolecular interaction energy (E_{int}^{sm}) at the MP2=full/6-311++G(2df,2p) level is also given in the table.

of the complex comes from the correlated part of the interaction energy in which dispersion is the main contributor. At $R = 2.60$ Å, the $E_{ind}^{(22)}$ and $E_{pol}^{(12)}$ are only −0.02 and −0.10 kcal/mol, respectively, for the HCl complex, and thus the dispersion is the main binding force at equilibrium. The major contribution to binding energy at the correlated level for the CH_4−HF complex also comes from the dispersion force because the contribution from the other two stabilizing components $E_{pol}^{(12)}$ and $E_{ind}^{(22)}$ are negligible at equilibrium. The importance of the dispersion force can be realized from a closer look at the Tables 3 and 4. At the Hartree−Fock level the interaction energy minima appear at $R = 2.60$ and 3.00 Å for the HF and HCl complexes, respectively, whereas inclusion of higher order (in terms of electron correlation) contributions to electrostatic, induction, exchange, and dispersion components (expressed as E_{int}^{corr}) brings the minima at $R = 2.40$ and 2.60 Å for the HF and

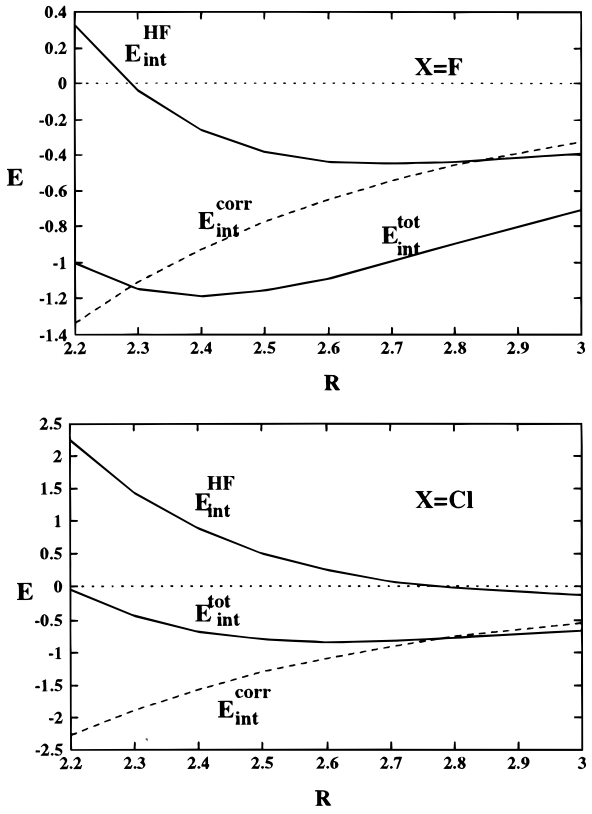

Figure 3. Change in Hartree−Fock interaction energy, correlation energy components of interaction energy, and total interaction energy (in kcal/mol) for the CH_4−HX (X = F, Cl) complex.

HCl complexes, respectively. But as already mentioned, at equilibrium, the contribution from induction and electrostatic components is negligible at correlated level for both the complexes and thus major contribution comes from dispersion. Figure 3 shows clearly the importance of dispersion forces in determining the minimum value of *R*. Nevertheless the importance of $\epsilon^{(1)}_{exch}$ should also be emphasized. Without this exchange contribution, the potential well at equilibrium would be overestimated by an amount of 0.32 and 0.17 kcal/mol for the HF and HCl complexes, respectively, which is 25% and 20% of their stabilization energy at equilibrium. This clearly shows the inadequacy of a Hartree−Fock plus dispersion (HFD) model, which neglects this important contribution. The interaction energy obtained from SAPT and BSSE corrected supermolecular calculations at the MP2=full/6-311++G(2df,2p) level is almost same. The optimum intermolecular distance *R* obtained from supermolecular calculations is shorter than the SAPT value. This is mainly due to the effect of BSSE during supermolecular calculations, which has been discussed in a previous section.

In view of the important role the dispersion forces played in these complexes, it is now clear that the basis set used in earlier studies[1,2,6] such as 6-311G(d,p) is not at all adequate for studying these types of complexes. To emphasize this point further, different energy components were calculated for the HF and HCl complexes of methane using another smaller basis set, 6-311++G(d,p). The results are listed in Table 5. At the Hartree−Fock level the contributions to the binding energy are almost same for both the basis sets. But dispersion contribution changes considerably on changing the basis set from 6-311++G(d,p) to 6-311++G(2df,2p) by as much as 33% and 38% for the HF and HCl complexes, respectively. This explains why the equilibrium *R* value decreases substantially with the increase

TABLE 5: Variation of Components of Interaction Energy (in kcal/mol) with the Change in Basis Set from 6-311++G(d,p) (Basis A) to 6-311++G(2df,2p) (Basis B) for the CH_4−HF (at R = 2.50 Å) and CH_4−HCl (at R = 2.70 Å) Complexes

	CH_4−HF		CH_4−HCl	
	Basis A	Basis B	Basis A	Basis B
E^{10}_{pol}	−0.77	−0.76	−0.60	−0.58
E^{10}_{exch}	1.15	1.12	1.05	1.02
$E^{20}_{ind,resp}$	−0.77	−0.82	−0.38	−0.39
E^{20}_{ex-ind}	0.24	0.23	0.17	0.16
E^{HF}_{int}	−0.30	−0.38	0.10	0.08
E^{2}_{disp}	−0.72	−0.96	−0.76	−1.05
E^{corr}_{int}	−0.50	−0.77	−0.63	−0.92
E^{tot}_{int}	−0.80	−1.15	−0.53	−0.84

TABLE 6: Components of Interaction Energy (in kcal/mol) for the (CH_4, HF) Dimer at the Bent Geometry[a] (Structure a in Figure 1) and at the Equilibrium Nonconventional Structure (Structure b in Figure 1 and R = 2.40 Å)[b]

	structure			structure	
	a	b		a	b
E^{10}_{pol}	−0.51	−0.93	E^{2}_{disp}	−0.64	−1.19
E^{10}_{exch}	1.06	1.62	E^{corr}_{int}	−0.44	−0.93
$E^{20}_{ind,resp}$	−0.36	−1.09	E^{tot}_{int}	−0.05	−1.19
E^{20}_{ex-ind}	0.27	0.34			
E^{HF}_{int}	0.39	−0.26	E^{sm}_{int}	−0.08	−1.27

[a] $H_a\cdots X$, 2.564 Å; $C\cdots H_b$, 3.338 Å; $\angle H_aCH_b$, 23°; $\angle CH_bF$, 101°. [b] BSSE corrected supermolecular interaction energy (E^{sm}_{int}) obtained at the MP2=full/6-311++G(3df,2p) level is given in the last row.

in basis set. SAPT analysis was also performed for the CH_4−HF system (at R = 2.40 Å) with 6-311++G(2d,2p) basis functions to observe the effect of the f-function on the components of energy. It was observed that all the major interaction energy components are insensitive to the addition of f-functions except $E^{(12)}_{pol}$ and $E^{(20)}_{disp}$, but their increment with the addition of f-function is only 0.04 kcal/mol. Thus at least in the present case, the presence of multiple d and p basis functions in the basis set is more important than higher angular momentum polarization function.

An interaction energy analysis for both the structures a and b (Figure 1) was performed for the (CH_4, HF) dimer. No equilibrium structure of bent geometry (like structure a in Figure 1) could be located from supermolecular calculations at the MP2=full/6-311++G(3df,2p) level. Structure b was found to be the most stable dimer at the said level of calculations. SAPT analysis was carried out assuming a bent structure having the same intermolecular coordinates as mentioned in ref 6 (which is almost similar to the experimental structure of ref 2). Monomer geometries were the same as mentioned earlier. The results are displayed in Table 6. At the Hartree−Fock level the structure b has a stabilization energy of −0.26 kcal/mol, whereas the bent dimer is energetically unstable by 0.39 kcal/mol. These results can be accounted for by the substantially lower $E^{(10)}_{pol}$ and $E^{(20)}_{ind}$ for the bent structure and their preponderance over the exchange forces. The dispersion component is also much lower for the conventional hydrogen-bonded structure leading to a large difference in their stabilization energy.

4. Conclusions

In the equilibrium geometry of all the (CH_4, HX), X = F, Cl, Br, dimers, the proton of H−X forms a hydrogen bond with the center of one of the tetrahedral faces of methane with a near C_{3v} symmetry. The conventional hydrogen-bonded structure in which the H-atom of methane forms a hydrogen bond with the fluorine of HF is much less stable, and at the MP2=full/6-311++G(3df,2p) level it is a transition state. In this context, it is interesting to mention the recent work on the CH_4−H_2O dimer.[19] It has been found that the *face approach* (similar to Figure 1b, see also Figure 1 of ref 19) gives rise to the most stable dimer. It was argued that the exchange repulsion is relatively small for the *face approach* compared to *edge* and *vertex approach*. This allows two monomers for a closer contact in the *face approach*, which gives rise to larger dispersion energy. The present conclusion on the dimeric structure of the (CH_4, HX) system that the *face approach* gives the most stable dimer is also along the same line. SAPT analysis shows that the attractive forces such as electrostatic, induction, and dispersion are much higher for the nonconventional hydrogen-bonded structure when the proton of HF faces the center of one of the tetrahedral faces of CH_4. SAPT analysis also shows that dispersion plays an important role in determining the equilibrium structure of these complexes.

Acknowledgment. A.K.C. thanks the Research Council of K.U., Leuven, for a postdoctoral fellowship. Thanks are also due to Prof. P. E. S. Wormer, University of Nijmegen, The Netherlands, for many helpful discussions.

References and Notes

(1) Davis, S. R.; Andrews, L. *J. Chem. Phys.* **1987**, *86*, 3765.

(2) Legon, A. C.; Roberts, B. P.; Wallwork, A. L. *Chem. Phys. Lett.* **1990**, *173*, 107.

(3) Ohshima, Y.; Endo, Y. *J. Chem. Phys.* **1990**, *93*, 6256.

(4) Atkins, M. J.; Legon, A. C.; Wallwork, A. L. *Chem. Phys. Lett.* **1992**, *192*, 368.

(5) Govender, M. G.; Ford, T. A. *J. Mol. Struct.: THEOCHEM* **1995**, *338*, 141.

(6) Nguyen, M. T.; Coussens, B.; Vanquickenborne, L. G.; Fowler, P. W. *Chem. Phys. Lett.* **1990**, *175*, 593.

(7) Chalasinski, G.; Szczesniak, M. M. *Chem. Rev.* **1994**, *94*, 1723.

(8) Frisch, M. J.; Trucks, G. W.; Schlegel, H. B.; Gill, P. M. W.; Johnson, B. G.; Robb, M. A.; Cheeseman, J. R.; Keith, T.; Petersson, G. A.; Montgomery, J. A.; Raghavachari, K.; Al-Laham, M. A.; Zakrzewski, V. G.; Ortiz, J. V.; Foresman, J. B.; Cioslowski, J.; Stefanov, B. B.; Nanayakkara, A.; Challacombe, M.; Peng, C. Y.; Ayala, P. W.; Chen, W.; Wong, M. W.; Andres, J. L.; Replogle, E. S.; Gomperts, R.; Martin, R. L.; Fox, D. J.; Binkley, J. S.; DeFrees, D. J.; Baker, J.; Stewart, J. P.; Head-Gordon, M.; Gonzalez, C.; Pople, J. A. *Gaussian 94*, Revision D.3; Gaussian, Inc.: Pittsburgh, PA, 1995.

(9) Jeziorski, B.; Chalasinski, G.; Szalewicz, K. *Int. J. Quantum Chem.* **1978**, *14*, 271.

(10) Jeziorski, B.; Moszynski, R.; Szalewicz, K. *Chem. Rev.* **1994**, *94*, 1887.

(11) Jeziorski, B.; Moszynski, R.; Ratkiewicz, A.; Rybak, S.; Szalewicz, K.; Williams, H. L. In *Methods and Techniques in Computational Chemistry: METECC-94, Vol. B, Medium Size Systems*; Clementi, E., Ed.; STEF: Cagliari, 1993; p 79.

(12) Boys, S. F.; Bernardi, F. *Mol. Phys.* **1970**, *19*, 553.

(13) Paulson, L. Ph.D. Thesis, University of Salford, UK, 1983. Barnes, A. J. *J. Mol. Struct.* **1983**, *100*, 259.

(14) Moszynski, R.; Korona, T.; Wormer, P. E. S.; van der Avoird, A. *J. Chem. Phys.* **1995**, *103*, 321.

(15) Moszynski, R.; Wormer, P. E. S.; van der Avoird, A. *J. Chem. Phys.* **1995**, *102*, 8385.

(16) Heijmen, T. G. A.; Korona, T.; Moszynski, R.; Wormer, P. E. S.; van der Avoird, A. *J. Chem. Phys.* **1997**, *107*, 902.

(17) Purvis III, G. D.; Bartlett, R. J. *J. Chem. Phys.* **1982**, *76*, 1910.

(18) Moszynski, R.; Wormer, P. E. S.; Jeziorski, B.; van der Avoird, A. *J. Chem. Phys.* **1994**, *101*, 2811.

(19) Szczesniak, M. M.; Chalasinski, G.; Cybulski, S. M.; Cieplak, P. *J. Chem. Phys.* **1993**, *98*, 3078.